FIBER INTERACTION IN A NERVE TRUNK

JOHN W. CLARK, JR. *and* ROBERT PLONSEY

From the Bioengineering Group, Electrical Engineering Department, Rice University, Houston, Texas 77001, and the Biomedical Engineering Department, Case Western Reserve University, Cleveland, Ohio 44106

ABSTRACT This paper is concerned with the nature of the transmembrane potential induced in an inactive nerve fiber lying in an impressed potential field within a nerve trunk. The impressed potential field is assumed to be produced by the synchronous activity of other fibers within the trunk; an expression for the induced transmembrane potential is obtained utilizing the principles of electromagnetic field theory. The results strongly indicate that membrane capacitance is the main determinant of the induced transmembrane potential wave form.

INTRODUCTION

Studies of nerve fiber interaction between two adjacent nerve fibers (one active, the other inactive) lying in a nerve trunk (Clark and Plonsey, 1970) have prompted a further investigation of the induced transmembrane potential in an inactive fiber when many active synchronous fibers lie in the same nerve trunk. While the dispersion seen in the compound action potential shows that ordinarily no significant interaction of fibers occurs, nevertheless it is important to quantitative studies to elucidate order of magnitude and dependence on geometrical and electrical parameters. Such studies are important in the investigation of pathological conditions since they may exclude or suggest ephaptic implication.

This problem can be immeasurably simplified by assuming that within a nerve trunk (*a*) the interstitial conductive medium confines the external current to axial flow only,[1] and (*b*) a large number of constituent fibers of the trunk are of equal diameter and simultaneously active. As a result, the interstitial potentials everywhere in a given transverse plane would be essentially the same and therefore, an inactive fiber lying in such a medium has an impressed potential field that is axially symmetric and a function only of axial distance z. We assume the existence of an action potential propagating in the negative z direction so that for any field quantity

[1] In the basic two-fiber interaction problem studied by Clark and Plonsey (1970), the spatial distribution of interstitial potential is found to be quite uniform, for nerve trunk radii in the physiologic range.

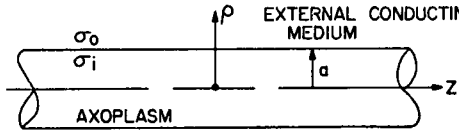

FIGURE 1 Cylindrical nerve fiber situated in a conducting bathing medium. A potential field $\Phi_e(z)$ is present in this medium and is given by equation 1.

$\psi(\rho, z, t)$ satisfies

$$\psi(\rho,z, t) = \psi(\rho, z + vt), \tag{1}$$

where v is the conduction velocity. For simplicity we shall suppress reference to the temporal variation but this can always be restored by replacing z by $(z + vt)$. We therefore specify an impressed potential $\Phi_e(z)$ at the outer membrane surface ($\rho = a$) of the inactive fiber (see Fig. 1). For mathematical convenience this surface potential may be represented as a sum of gaussian potential distributions (Clark and Plonsey, 1966), that is:

$$\Phi_e(z) = \sum_{i=1}^{m} A_i \quad \exp \quad [-B_i^2(z - D_i)^2]. \tag{2}$$

The axoplasmic medium of the inactive fiber is assumed to be homogeneous and isotropic, and to possess a specific conductivity σ_i (mho/cm). The interstitial medium is also assumed to be uniform possessing a specific conductivity σ_0 (mho/cm). The fiber membrane is assumed to possess a membrane conductance $\bar{\sigma}_m$ (mho/cm^2) and capacitance $\bar{C}_m$ (μF/cm^2). This paper will be especially concerned with the effect of variations in membrane conductance and capacity on the magnitude and waveshape of the transmembrane potential.

EXPRESSION FOR POTENTIAL AXOPLASMIC MEDIUM

The general expression for axoplasmic potential $\Phi^i(\rho, z)$, obtained as a solution of Laplace's equation in the cylindrical axoplasmic medium ($0 \leq \rho \leq a$) under the assumed conditions of axial symmetry is

$$\Phi^i(\rho, z) = \int_{-\infty}^{\infty} E(k) I_0(|k|\rho) e^{-jkz}\, dk, \tag{3}$$

where I_0 is the modified Bessel function of the first kind and $E(k)$ is an, as yet, undetermined function. Considering the inactive fiber membrane as a distributed, parallel resistance-capacitance network, the appropriate expression for transmembrane current density $J_m(z)$ (amp/cm^2) is:

$$J_m(z) = \bar{\sigma}_m \Phi_m(z) + \bar{C}_m \frac{\partial \Phi_m(z)}{\partial t}. \tag{4}$$

In equation 4, Φ_m is the transmembrane potential, defined as:

$$\Phi_m(z) = \Phi^i(a, z) - \Phi_e(z). \tag{5}$$

The time derivative in equation 4 may be evaluated, since equation 1 requires that

$$\frac{\partial \psi}{\partial t} = v \frac{\partial \psi}{\partial z}. \tag{6}$$

Thus, equation 4 becomes:

$$J_m(z) = \bar{\sigma}_m \Phi_m(z) + v\bar{C}_m \frac{\partial \Phi_m}{\partial z}. \tag{7}$$

BOUNDARY CONDITIONS AT $\rho = a$

The appropriate boundary condition at the inactive fiber membrane surface is expressed mathematically as:

$$J_m(z) = -\sigma_i \left.\frac{\partial \Phi^i}{\partial \rho}\right|_{\rho=a}, \tag{8}$$

where J_m is the transmembrane current density. This equation is simply an expression of the continuity of current crossing the membrane. Since the membrane is characterized electrically as a distributed resistance-capacitance network the transmembrane current density J_m is also given by equation 4. Thus, substituting equation 4 into equation 8, one obtains

$$\sigma_i \left.\frac{\partial \Phi^i}{\partial \rho}\right|_a + \bar{\sigma}_m \Phi_m(z) + v\bar{C}_m \frac{\partial \Phi_m}{\partial z} = 0. \tag{9}$$

Equation 9 is the equation utilized in the solution for the unknown function $E(k)$ in equation 3.

APPLICATION OF BOUNDARY CONDITION—SOLUTION FOR UNDETERMINED POTENTIAL FUNCTION

In obtaining a solution for $E(k)$, an expression for transmembrane potential is first obtained from equation 5.

$$\Phi_m(z) = \int_{-\infty}^{\infty} E(k) I_0(|k|a) e^{-jkz}\, dk - \Phi_s(z), \tag{10}$$

where the specified surface potential distribution $\Phi_s(z)$ is given by equation 1. This distribution may, however, be represented by its Fourier transform; that is,

$$\Phi_s(z) = \frac{1}{2\pi} \int_{-\infty}^{\infty} F_s(k) e^{-jkz}\, dk, \tag{11}$$

$$F_s(k) = \int_{-\infty}^{\infty} \Phi_s(z) e^{jkz}\, dz, \tag{12}$$

where $F_s(k)$ is defined as the Fourier transform of $\Phi_s(z)$. The Fourier transform may

be evaluated by direct integration (Clark and Plonsey, 1966) to be

$$F_s(k) = \sqrt{\pi} \sum_{i=1}^{m} \frac{A_i}{B_i} \exp[-k^2/4B_i^2] \exp[jkD_i]. \quad (13)$$

Thus, upon substitution of equation 11 into equation 10, the expression for Φ_m becomes:

$$\Phi_m(z) = \frac{1}{2\pi} \int_{-\infty}^{\infty} [2\pi E(k) I_0(|k|a) - F_s(k)] e^{-jkz}\, dk. \quad (14)$$

Upon substitution of equation 14 into equation 7, the expression for transmembrane current density becomes:

$$J_m(z) = \frac{\bar{Y}_m}{2\pi} \int_{-\infty}^{\infty} [2\pi E(k) I_0(|k|a) - F_s(k)] e^{-jkz}\, dk, \quad (15)$$

where $\bar{Y}_m$ is defined as:

$$\bar{Y}_m \equiv \bar{\sigma}_m - jk\nu\bar{C}_m. \quad (16)$$

Thus, equation 9 becomes:

$$0 = \int_{-\infty}^{\infty} \left[\sigma_i |k| E(k) I_1(|k|a) + \frac{\bar{Y}_m}{2\pi} (2\pi E(k) I_0(|k|a) - F_s(k)) \right] e^{-jkz}\, dk. \quad (17)$$

If the integral of equation 17 is zero over the limits $(-\infty, \infty =$, it follows that:

$$\left[\sigma_i |k| E(k) I_1(|k|a) + \frac{\bar{Y}_m}{2\pi} (2\pi E(k) I_0(|k|a) - F_s(k)) \right] = 0. \quad (18)$$

Thus,

$$E(k) = \frac{F_s(k)}{2\pi} \frac{\bar{Y}_m}{[\sigma_i |k| I_1(|k|a) + \bar{Y}_m I_0(|k|a))]}. \quad (19)$$

Since $\bar{Y}_m$ is defined according to equation 16, the expression for $E(k)$ is also complex and may be written in the form:

$$E(k) = \frac{F_s(k)}{2\pi} \left[\frac{x_3(k) + jx_4(k)}{(x_1(k))^2 + (x_2(k))^2} \right], \quad (20)$$

where

$$x_1(k) = \sigma_i |k| I_1(|k|a) + \bar{\sigma}_m I_0(|k|a), \quad (21)$$

$$x_2(k) = +k\nu\bar{C}_m I_0(|k|a), \quad (22)$$

$$x_3(k) = \bar{\sigma}_m x_1(k) + kv\bar{C}_m x_2(k), \tag{23}$$

$$x_4(k) = \bar{\sigma}_m x_2(k) - kv\bar{C}_m x_1(k). \tag{24}$$

Thus, substituting equation 20 into equation 14

$$\Phi_m(z) = \frac{1}{2\pi}\int_{-\infty}^{\infty} F_s(k)\left[\frac{(x_3 + jx_4)}{x_1^2 + x_2^2} I_0(|k|a) - 1\right] e^{-jkz}\, dk. \tag{25}$$

Substituting equation 13 into equation 25, one obtains

$$\Phi_m(z) = \frac{1}{\sqrt{2\pi}}\int_{-\infty}^{\infty}\sum_{i=1}^{m}\frac{A_i}{B_i}\exp\left[-k^2/4B_i^2\right] \cdot\left[\frac{(x_3 + jx_4)}{x_1^2 + x_2^2} I_0(|k|a) - 1\right]\exp\left[-jk(z - D_i)\right] dk. \tag{26}$$

One will note from the definitions of x_1, x_2, x_3, and x_4 above that x_1 and x_3 are even functions of k, while x_2 and x_4 are odd functions of k. The exponential term $\exp\left[-k^2/4B_i^2\right]$ and the modified Bessel function $I_0(|k|a)$ will also be found to be even functions of k. As a result, equation 26 may be rewritten as:

$$\Phi_m(z) = 1/\sqrt{\pi}\int_0^{\infty}\sum_{i=1}^{m}\frac{A_i}{B_i}\exp\left[-k^2/4B_i^2\right]\left[\left(\frac{x_3}{x_1^2 + x_2^2} I_0(ka) - 1\right) \cdot\cos k(z - D_i) + \frac{x_4}{x_1^2 + x_2^2} I_0(ka)\sin k(z - D_i)\right] dk. \tag{27}$$

Letting $y \equiv ka$

$$\Phi_m(z) = \frac{1}{\sqrt{\pi}a}\int_0^{\infty}\sum_{i=1}^{m}\frac{A_i}{B_i}\exp\left[-y^2/4a^2B_i^2\right]\left[\left(\frac{x_3 I_0(y)}{x_1^2 + x_2^2} - 1\right) \cdot\cos\left(y\,\frac{(z - D_i)}{a}\right) + \frac{x_4}{x_1^2 + x_2^2} I_0(y)\sin\left(y\,\frac{(z - D_i)}{a}\right)\right], \tag{28}$$

where

$$x_1(y) = \frac{\sigma_i y I_1(y)}{a} + \bar{\sigma}_m I_0(y), \tag{29}$$

$$x_2(y) = \frac{yv\bar{C}_m}{a} I_0(y), \tag{30}$$

$$x_3(y) = \bar{\sigma}_m x_1(y) + \frac{yv\bar{C}_m}{a} x_2(y), \tag{31}$$

$$x_4(y) = \bar{\sigma}_m x_2(y) - \frac{yv\bar{C}_m}{a} x_1(y). \tag{32}$$

SYNTHETIC DATA

Since equation 28 is too complex to permit a general solution, we proceed by choosing a representative problem for which Φ_m can be evaluated and effects of $\bar{r}_m(= 1/\bar{\sigma}_m)$ and $\bar{C}_m$ on transmembrane potential studied. In spite of this seemingly restrictive approach, certain generalizations will be seen to be suggested by the results.

For simplicity, the form of the impressed surface potential at the inactive fiber $\Phi_s(z)$ is represented by a single gaussian distribution, that is, using the nomenclature of equation 1 we have

$$\Phi_s(z) = A_1 \quad \exp \quad [-B_1^2(z - D_1)^2]. \tag{33}$$

The representative value of the amplitude factor A_1 was chosen to be 10 mv. This value is in the order of magnitude of expected values and should be considered as simply a reference (normalized) quantity.

The values chosen for B_1 and D_1 in equation 1 are

$$B_1 = 4.0 \text{ cm}^{-1}, \qquad D_1 = 0.0 \text{ cm},$$

while the values chosen for the geometrical and electrical parameters of the model are:

(1)	$a = 10\ \mu$	(fiber radius)
(2)	$\bar{r}_m = 1/\bar{\sigma}_m = 2000\ \Omega \cdot \text{cm}^2$	(resistance per unit area of membrane)
(3)	$\bar{C}_m = 0.8\ \mu F/\text{cm}^2$	(capacitance per unit area of membrane)
(4)	$\sigma_i = 1/90\ \Omega \cdot \text{cm}$	(specific conductivity of axoplasm)
(5)	$v = 1000$ cm/sec	(conduction velocity of active wave front).

Approximations in the numerical evaluation of equation 28 are essentially the same as those discussed in Clark and Plonsey (1968). The limits of integration used are (0, 0.14) and are obtained by evaluating and plotting the integral of equation 28 so as to determine an upper bound on y, the variable of integration. A Burroughs 5500 digital computer (Burroughs Corp., Detroit, Mich.) was utilized in this study.

RESULTS

The transmembrane potential distribution $\Phi_m(z)$ of an inactive fiber placed in the impressed field described in Fig. 2, was calculated for the aforementioned (typical) values of membrane resistance and capacitance. The result is shown in Fig. 3 and reveals an essentially diphasic curve that has a peak-to-peak value of approximately 450 μv. Fig. 3 also contains curves for transmembrane potential at other values of $\bar{r}_m$ ranging from 500 to 100,000 $\Omega \cdot \text{cm}^2$, hence covering the physiological range of values (1000–4000 $\Omega \cdot \text{cm}^2$). One notes that the results are not very sensitive to changes in $\bar{r}_m$ and thus suggests that $\bar{C}_m$ may be the controlling parameter. The curve for $\bar{r}_m = 100{,}000\ \Omega \cdot \text{cm}^2$ might be considered as representing the type of behavior

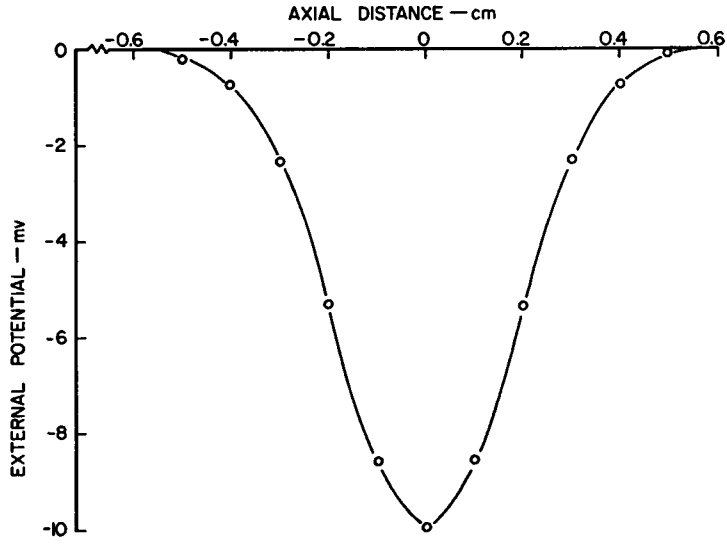

FIGURE 2 Assumed potential distribution $\Phi_s(z)$.

that would arise from a fiber possessing an essentially pure capacitive membrane since the resistive part is in the nature of an open circuit.

When $\bar{r}_m$ is held constant at 2000 $\Omega \cdot cm^2$ and $\bar{C}_m$ is varied over the range ($0.3 \leq \bar{C}_m \leq 1.2$ $\mu F/cm^2$), the wave shape remains essentially diphasic as seen in the curves of Fig. 4. Here the membrane behavior appears to be clearly dominated by the membrane capacitance. One notes from Fig. 4, that the peak magnitude of Φ_m is roughly inversely proportional to $\bar{C}_m$ over the range of values considered.

The case where $\bar{C}_m = 0.01$ $\mu F/cm^2$ is shown in Fig. 5; the curve for $\bar{C}_m = 0.6$ $\mu F/cm^2$ is presented for contrast (note that these curves are plotted to different scales). The $\bar{C}_m = 0.01$ $\mu F/cm^2$ curve might be expected to characterize the "resistive" membrane since the capacitance is very small. It differs from the "capacitive" membrane in that its wave shape is triphasic and its magnitude much larger.

From Figs. 3–5, and a knowledge of the physiological ranges of the parameters $\bar{r}_m$ and $\bar{C}_m$ ($1000 \leq \bar{r}_m \leq 4000$ $\Omega \cdot cm^2$; $0.5 \leq \bar{C}_m \leq 1.2$ $\mu F/cm^2$) it is clear that the main determinant of the wave shape of the induced transmembrane potential is the membrane capacitance. Fig. 6 indicates that the magnitude of transmembrane potential increases linearly with fiber radius under the assumption that all other model parameters remain invariant over the range of radii considered.

While the numerical results apply to the specific model it is possible to readily apply them to a variety of additional conditions. Thus it should be noted that the assumed interstitial action potential amplitude of 10 mv is a multiplicative constant in all computations. Should this value actually be 50 mv then all resultant curves would apply provided the ordinate scale were multiplied by 5. In this connection, if r_e is the net interstitial resistance per unit length, r_i the resistance per unit length of a

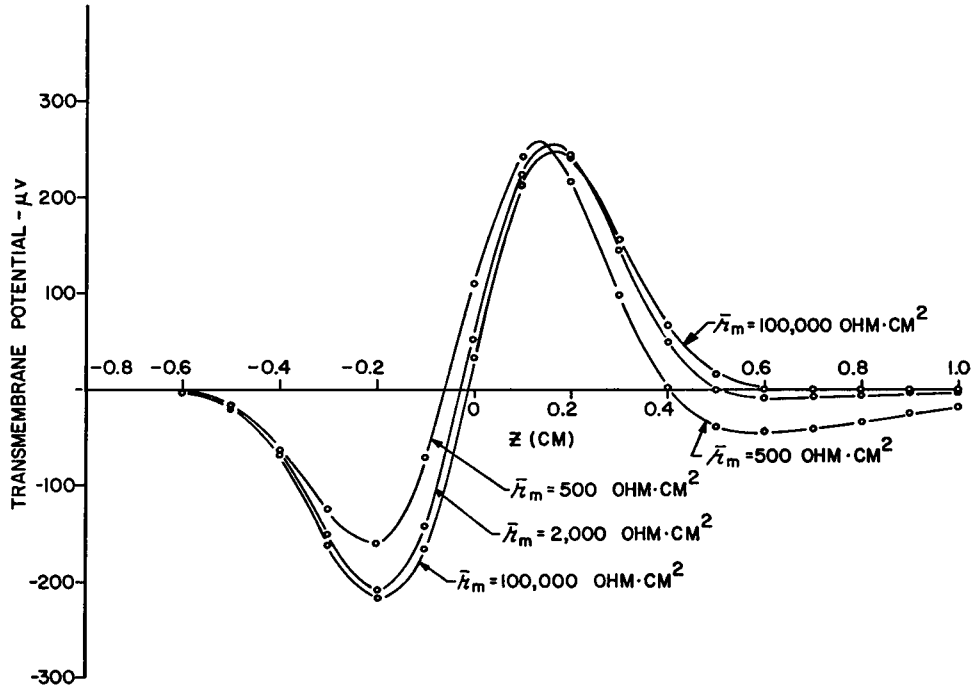

FIGURE 3 Transmembrane potential as a function of axial distance z for various values of membrane resistance. The value of $\bar{C}_m$ is 0.8 μF/cm^2 in all cases.

single fiber, and N the number of synchronously active fibers, then (Patlak, 1955; Lorente de No, 1947)

$$\Phi_e = (1 + r_i/Nr_e)^{-1}\Phi_m .$$

The result depends on N but it is reasonable to expect conditions for which the coefficient of Φ_m would lie between 0.1 and 0.7 yielding Φ_e somewhere between 10 and 70 mv.

The conduction velocity enters the computation only as a product with the membrane capacitance. Consequently the potential fields on and within the inactive fiber are unchanged if the $v\bar{C}_m$ product is held constant. Thus the curves of Fig. 4 can be applied to other values of v than the assumed 10 m/sec provided the same $v\bar{C}_m$ obtains.

As revealed by Fig. 6 the transmembrane potential in the inactive fiber is directly proportional to the diameter. Thus for diameters other than the assumed 10 μ a simple scaling can be accomplished.

As an illustration of the above consider a bundle of muscle fibers of 50 μ diameter with Φ_e = 70 mv, $\bar{C}_m$ = 5 μF/cm^2, and v = 1.6 m/sec (Katz, 1948). From the $v\bar{C}_m$ product we see that the $\bar{C}_m$ = 0.8 μF/cm^2 curves of this paper apply. Since the am-

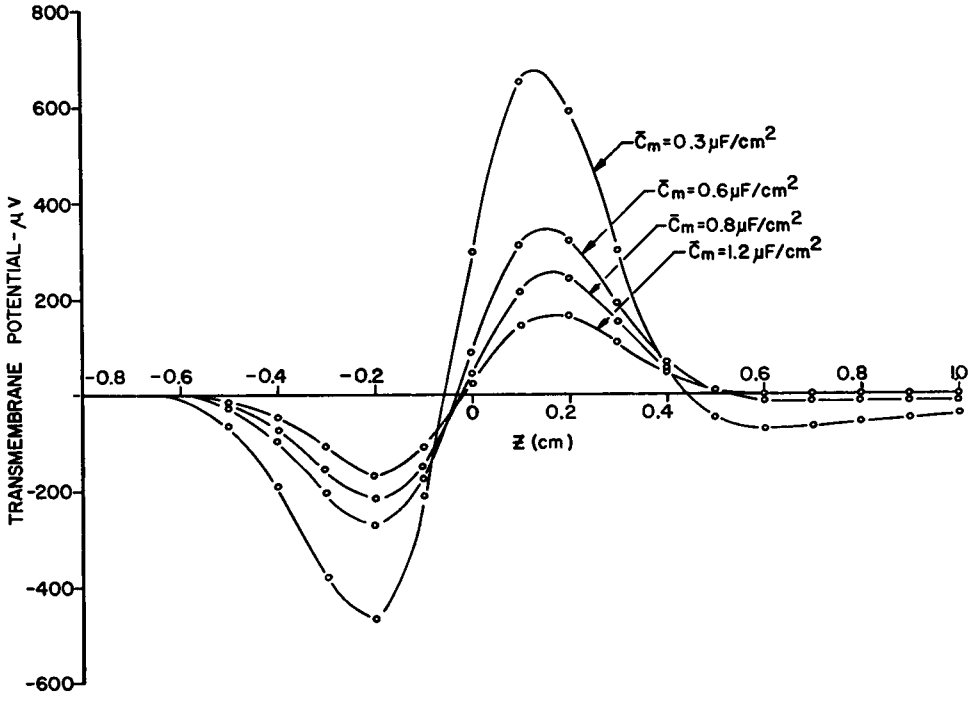

FIGURE 4 Transmembrane potential as a function of z for various values of membrane capacitance in the range ($0.3 \leq \bar{C}_m \leq 1.2$ μF/cm²). The value of $\bar{r}_m$ was held constant at 2000 Ω·cm².

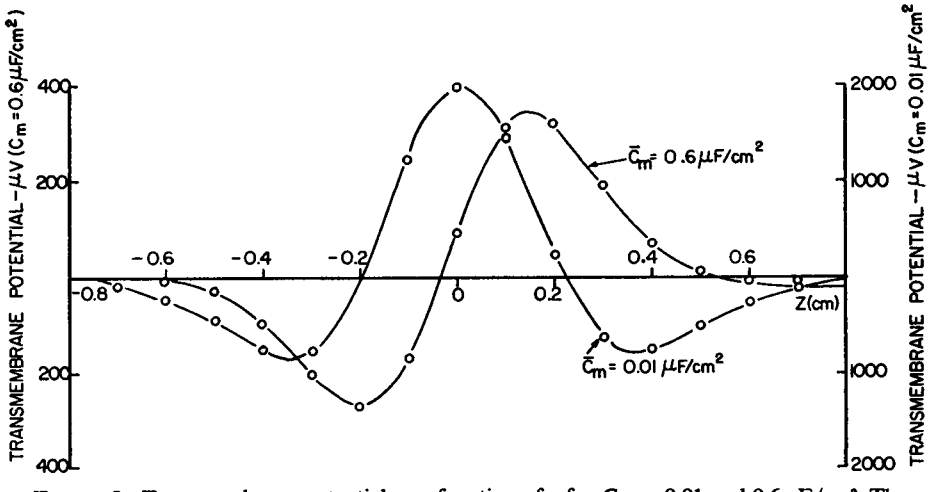

FIGURE 5 Transmembrane potential as a function of z for C_m = 0.01 and 0.6 μF/cm². The value of $\bar{r}_m$ is 2000 Ω·cm² in both cases.

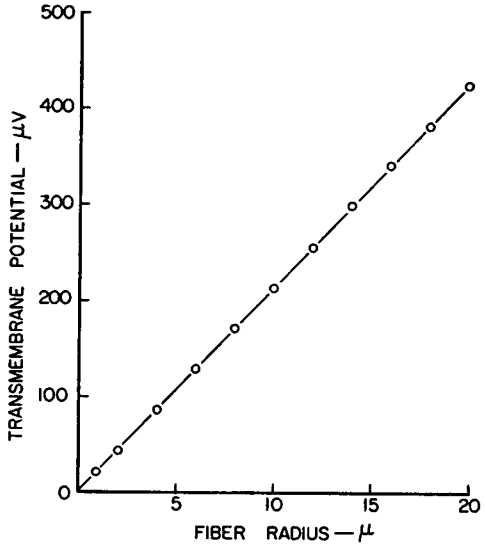

FIGURE 6

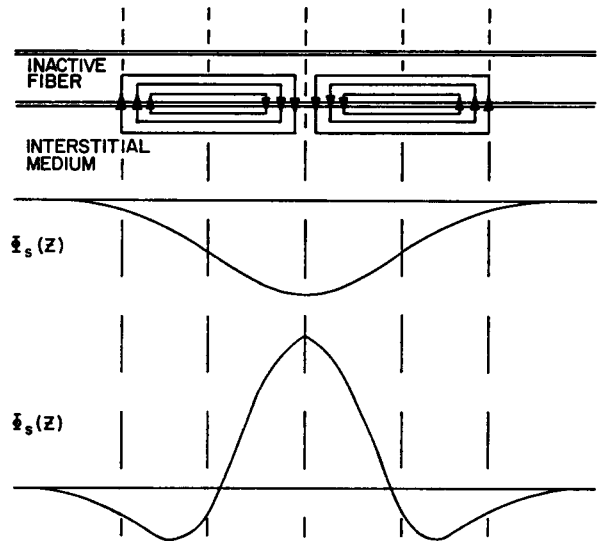

FIGURE 7

FIGURE 6 Induced transmembrane potential Φ_m as a function of fiber radius in the plane $z = -0.2$ cm.

FIGURE 7 Analysis of current flow and transmembrane potential for an inactive resistive membrane.

plitude and diameter factors are multiplicative the peak-induced transmembrane potential is $0.25 \times 7 \times 5 = 8.7$ mv.

DISCUSSION

The wave forms which result for the resistive and capacitive membranes are not too difficult to explain. For the resistive case ($\bar{C}_m$ very small) illustrated in Fig. 7, the interstitial potential is negative at the center and zero to the right and left. The resultant current density field depends only on the instantaneous potential field (all fields being quasi-static). Consequently $J_m(z)$ has a triphasic wave form and its direction is into the inactive fiber at the "right" and "left" and out of the fiber at the center as shown in Fig. 7. Since the membrane is purely resistive, the transmembrane potential is proportional to $J_m(z)$ according to equation 7. That is,

$$\Phi_m(z) = J_m(z)/\bar{\sigma}_m \,. \tag{34}$$

For the capacitive membrane ($\bar{r}_m$ very large, or conversely, $\bar{\sigma}_m$ very small) we shall assume that the current flowing into and out of the inactive fiber has essentially the same pattern as for the resistive membrane. That is, we assume the inactive fiber, as an electrical load, to be mainly characterized by its high axoplasmic resistance and therefore to remain essentially the same resistive load regardless of

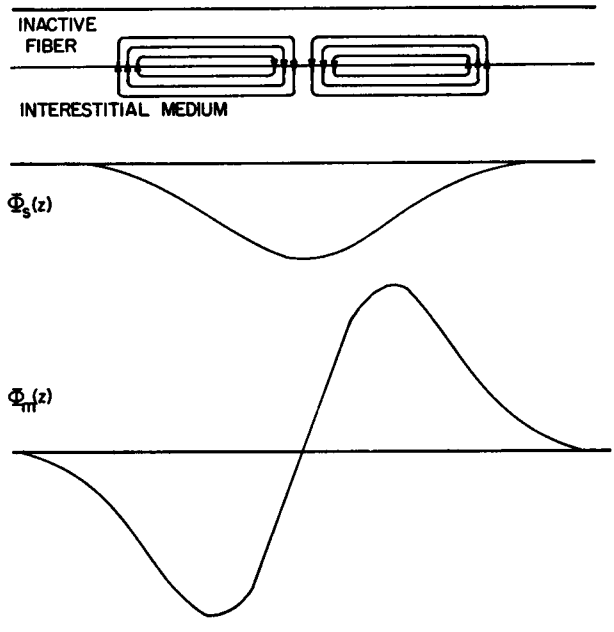

FIGURE 8 Current flow and transmembrane potential for an inactive fiber with capacitive membrane.

changes in membrane parameters. The aforementioned assumption depends on the effective axoplasmic resistance to greatly exceed the effective membrane impedance in the range of interest. We shall return to this with some quantitative measure presently. Now even though the current linking the inactive fiber is the same for the capacitive membrane as for the resistive membrane, the transmembrane potentials will not be similar. This comes about because the potential developed across a capacitance is not proportional to the current through it, but rather to its time integral. This is clearly seen from a consideration of equation 7 for the capacitive case, that is

$$\Phi_m(z) = (1/v\bar{C}_m) \int J_m(z)\, dz. \tag{35}$$

Since $J_m(z)$ has a triphasic wave form, transmembrane potential in this case will be diphasic in nature (see Fig. 8).

Thus the "capacitive" membrane possesses a diphasic transmembrane potential whereas the "resistive" membrane possesses a triphasic wave form for $\Phi_m(z)$. For intermediate cases, that is, for values of $\bar{r}_m$ and $\bar{C}_m$ in the physiologic range, Figs. 3–5 clearly indicate that the prime determinant of transmembrane potential is membrane capacitance.

A rough model which permits one to deduce (also very roughly) some quantitative relationships can be put together as follows. First we can think of the applied poten-

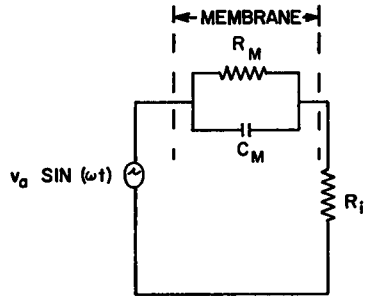

FIGURE 9 Lumped equivalent circuit for inactive fiber with *RC* membrane.

tial field $\Phi_e(z)$ as constituting a single sine wave; we assume it to be the output of an AC generator. The passive fiber can be thought of as an electrical network to which the AC generator is connected. The former will be represented by a parallel combination of membrane capacitance and resistance in series with the axoplasmic resistance. While the network is truly a distributed one the suggested lumped equivalents are proposed for simplicity. To compute an effective surface area of membrane we define a characteristic length λ as the distance between points of maximum slope of $\Phi_e(z)$. This corresponds to a half-spatial cycle, considering the applied potential to constitute a full spatial cycle. The network is described in Fig. 9 where R_M is the total membrane resistance, C_M the total membrane capacitance, and R_i the longitudinal axoplasmic resistance of the fiber of length λ. The applied voltage v_a has the magnitude equal to the maximum value of $\Phi_e(z)$ while ω is calculated from λ and the velocity of propagation v by

$$\omega = \frac{2\pi}{T} = \frac{2\pi v}{2\lambda} = \frac{\pi v}{\lambda}. \tag{36}$$

Using the values given previously we get

$$\begin{aligned} \lambda &= 0.4 \text{ cm}, \\ \omega &= 7850 \text{ rad/sec}, \\ C_M &= (0.8)(2\pi a\lambda) = 0.002 \ \mu\text{F}, \\ 1/\omega C_M &= 63.7 \text{ k}\Omega, \\ R_M &= \bar{r}_m/(2\pi a\lambda) = 800 \text{ k}\Omega, \\ R_i &= 90\lambda/(\pi a^2) = 11.4 \text{ M}\Omega. \end{aligned}$$

The numerical values tend to confirm several of the results already noted. First $1/(\omega C_M) \ll R_M$ hence demonstrating the membrane to be normally capacitive; that is since the shunt capacitive reactance is much smaller than the shunt resistance the membrane capacitance is predominant. Second, since $R_i \gg 1/(\omega C_M)$ the total load is essentially resistive over the range of values considered. The transmembrane

potential peak value, Φ_m, should be roughly given by

$$\Phi_m = \frac{v_a \left(\dfrac{1}{j\omega C_M + R_M^{-1}} \right)}{\dfrac{1}{i\omega C_M + R_M^{-1}} + R_i}, \tag{37}$$

which corresponds to the voltage division performed in the circuit of Fig. 9. The capacitive membrane is characterized by $1/(\omega C_M) \ll R_M$ hence $\bar{C}_m = 1/(\bar{r}_m\omega)$. In our example $\bar{r}_m = 2000\ \Omega\cdot\text{cm}^2$ and $0.6 < \bar{C}_m < 1.2\ \mu\text{F/cm}^2$ clearly satisfy the requisite inequality. In this case the above equation simplifies to

$$\Phi_m = \frac{v_a}{\omega C_M R_i} \tag{38}$$

and we note that Φ_m is inversely proportional to C_M and correlates reasonably well with results shown in Fig. 5. Using the specific values of $\bar{C}_m = 0.8\ \mu\text{F/cm}^2$, $\bar{r}_m = 2000\ \Omega\cdot\text{cm}^2$ gives a value of Φ_m/v_a of 0.005 which, however, does not compare too well with the value obtained from Fig. 3 of 0.024. This result also confirms an insensitivity to larger values of $\bar{r}_m$ as revealed in Fig. 3.

The resistive membrane is defined by the condition $R_M \ll 1/(\omega C_M)$, hence for $\bar{r}_m = 2000\ \Omega\cdot\text{cm}^2$, $\bar{C}_m \leq 0.01\ \mu\text{F/cm}^2$ is required. If $\bar{C}_m = 0.01\ \mu\text{F/cm}^2$, then $1/(\omega C_M) = 5.1\ \text{M}\Omega$ and the membrane will be primarily resistive. In this case the expression for Φ_m reduces to (approximately)

$$\Phi_m = \frac{R_M v_a}{R_i + R_M}.$$

Utilizing the values given we get

$$\Phi_m/v_a = 0.065.$$

This compares with the measured peak values (see Fig. 5) of 0.077, 0.196, and 0.076.

Although we have used numerical values to illustrate the simplified membrane model, it should be emphasized that only qualitative relations can rightfully be expected. It is indeed somewhat surprising that the results appear to have some quantitative predictability. This model while of an instructional type should nevertheless be helpful in providing an intuitive understanding of a particular type of fiber interaction.

ADDITIONAL COMMENTS

This paper, through a numerical example, gives the order of magnitude of voltage induced in an inactive fiber which lies in a bundle of active fibers and describes its dependence on electrical and geometrical parameters. In particular we see that the

ephaptic excitation of nerve fibers is rather unlikely in view of the low resultant transmembrane potentials unless the membrane should have an abnormally low capacitance (and high resistance). The possibility of interaction is less likely for very small fibers.

The results in this paper apply to inactive *unmyelinated* nerve fibers only. However, they also apply to bundles of skeletal muscle fibers and can serve to estimate the likelihood that excitation of a portion of the bundle will cause excitation of the remainder of the bundle. The brief example given at the conclusion of the Results section shows this to be a very real possibility since the values chosen are quite typical.

We have not considered interaction between two active fibers but from a qualitative standpoint the region just ahead of the action potential on the slower of the two is under the influence of its own local circuit current and the induced transmembrane potential of the faster conducting fiber. In this case even though the induced potentials are subthreshold they, nevertheless, contribute to a reduction in latency, hence increase in velocity, of the slower fiber. The degree of interaction depends on the relative strength and difference in intrinsic velocities.

The source of applied field on an inactive fiber may also arise from a stimulating (polarizing) current. The model should still be appropriate provided λ is related to the conventional space constant. Fig. 6 would then be interpreted as predicting increased excitability to *external* excitation for the larger diameter fibers in a nerve trunk. A linear relationship between excitability and diameter is expected.

SUMMARY

This paper is concerned with the nature of the transmembrane potential induced in an impressed potential field within a nerve trunk. The impressed potential field is assumed to be produced by the synchronous activity of other fibers within the trunk. An expression for the induced transmembrane potential is derived, and numerically evaluated utilizing typical physiological values for the constants of the mathematical model. The results strongly indicate that membrane capacitance plays a dominant role in the determination of the induced transmembrane potential wave form.

This research was supported by Public Health Service Grant 5 SO4 FR 06136-02 from the Division of Research Facilities and Resources, and Public Health Service Grant HE 10417.

Received for publication 17 December 1969 and in revised form 22 October 1970.

REFERENCES

CLARK, J. W., and R. PLONSEY. 1966. *Biophys. J.* **6**:95.
CLARK, J. W., and R. PLONSEY. 1968. *Biophys. J.* **8**:842.
CLARK, J. W., and R. PLONSEY. 1970. *Biophys. J.* **10**:937.
KATZ, B. 1948. *Proc. Roy. Soc. Ser. B. Biol. Sci.* **135**:506.
LORENTE DE NO, R. 1947. *Stud. Rockefeller Inst. Med. Res.* **131**:483.
PATLAK, C. S. 1955. *Bull. Math. Biophys.* **17**:287.